

Solving the Martian meteorite age conundrum using micro-baddeleyite and launch-generated zircon

D. E. Moser¹, K. R. Chamberlain², K. T. Tait³, A. K. Schmitt⁴, J. R. Darling^{1†}, I. R. Barker¹ & B. C. Hyde³

Invaluable records of planetary dynamics and evolution can be recovered from the geochemical systematics of single meteorites¹. However, the interpreted ages of the ejected igneous crust of Mars differ by up to four billion years^{1–6}, a conundrum⁷ due in part to the difficulty of using geochemistry alone to distinguish between the ages of formation and the ages of the impact events that launched debris towards Earth. Here we solve the conundrum by combining *in situ* electron-beam nanostructural analyses and U–Pb (uranium–lead) isotopic measurements of the resistant micromineral baddeleyite (ZrO₂) and host igneous minerals in the highly shock-metamorphosed shergottite Northwest Africa 5298 (ref. 8), which is a basaltic Martian meteorite. We establish that the micro-baddeleyite grains pre-date the launch event because they are shocked, cogenetic with host igneous minerals, and preserve primary igneous growth zoning. The grains least affected by shock disturbance, and which are rich in radiogenic Pb, date the basalt crystallization near the Martian surface to 187 ± 33 million years before present. Primitive, non-radiogenic Pb isotope compositions of the host minerals, common to most shergottites^{1–4}, do not help us to date the meteorite, instead indicating a magma source region that was fractionated more than four billion years ago^{9–12} to form a persistent reservoir so far unique to Mars^{1,9}. Local impact melting during ejection from Mars less than 22 ± 2 million years ago caused the growth of unshocked, launch-generated zircon and the partial disturbance of baddeleyite dates. We can thus confirm the presence of ancient, non-convecting mantle beneath young volcanic Mars, place an upper bound on the interplanetary travel time of the ejected Martian crust, and validate a new approach to the geochronology of the inner Solar System.

A puzzle in Martian science is that basaltic shergottites yield whole-rock and non-radiogenic mineral Pb–Pb isotopic compositions consistent with a primary Noachian (approximately four billion years (Gyr) ago) age for crystallization⁴, whereas mineral isochrons consistently return ‘young’ late-Amazonian (<0.6 Gyr) ages^{1–3}. Resolution of this shergottite ‘age conundrum’⁷ by U–Pb dating of microcrystals of the accessory phase baddeleyite (ZrO₂) has been pursued^{5,6}, although the small target sizes pose technical challenges. Questions persist as to whether the young dates reflect magmatism or disturbance by metamorphic events on Mars, including shock metamorphism before and during meteorite ejection^{4,7}. Shock experiments aimed at resolving the conundrum predict that shock unloading and the attendant heating do not cause significant Pb-loss from baddeleyite, although it is acknowledged that experiment shock loading paths may not be entirely analogous to nature¹³. Similar experiment-based predictions were made for the mineral zircon, but these did not apply to natural samples where shock heating and related fluid activity were significant^{14,15}. Here we combine *in situ* U–Pb and Pb–Pb isotopic analyses, including the recently developed technique of secondary ion mass-spectrometry (SIMS) micro-baddeleyite dating^{16,17}, with chemical and microstructure data obtained with electron nanobeam techniques including cathodoluminescence and

electron backscatter diffraction (EBSD) that can reveal baddeleyite paragenesis and degree of alteration by shock processes¹⁵ before dating. We have focused on micro-baddeleyites from shergottite NWA 5298 (ref. 8), accession number M53387 from the Royal Ontario Museum’s meteorite collection, one of the most highly shocked shergottites, to demonstrate our methodology for resolving primary and shock-related age records.

Meteorite NWA 5298 is an enriched basaltic (diabasic) shergottite exhibiting a primary igneous texture, which, apart from its relatively oxidized state, is chemically similar to other basaltic shergottites including Shergotty, Zagami and Los Angeles⁸. It is an unbrecciated, highly shocked igneous rock that probably crystallized from a thick lava flow. Partial breakdown of pyroxferroite to fayalite suggests reheating by a later event such as overlying lava flow or shock heating⁸.

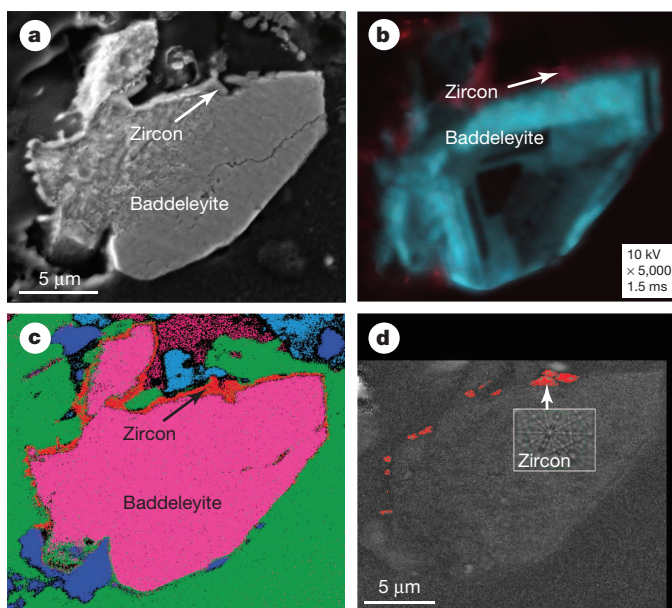


Figure 1 | Nanostructural data for Martian baddeleyite grains showing igneous growth zoning, shock state and launch-generated reaction rim of unshocked zircon. **a**, Secondary electron micrograph of euhedral micro-baddeleyite Grain 16 after partial (upper left) ablation by SIMS. We note its granular texture, caused by shock metamorphism. **b**, Cathodoluminescence image revealing planar trace-element banding typical of igneous crystallization, and zircon rim (magenta) on the side of the grain nearest to a quenched melt pocket. **c**, False-colour element map based on X-ray energy dispersive spectroscopy showing baddeleyite (pink), zircon rim (red) and host maskelynite (green). **d**, EBSD band contrast (diffraction signal strength) map (50 nm step size) indicating weak diffraction in all phases, owing to shock, except for the unshocked zircon rim crystallites (red) that grew during the launch from Mars (the inset shows a representative electron backscatter diffraction pattern for zircon).

¹Department of Earth Sciences, University of Western Ontario, 1151 Richmond Street, London, Ontario N6A 5B7, Canada. ²Department of Geology and Geophysics, University of Wyoming, 1000 East University Avenue, 3006, Laramie, Wyoming 82071, USA. ³Department of Natural History, Mineralogy, Royal Ontario Museum, Toronto, Ontario M5S 2C6, Canada. ⁴Department of Earth and Space Sciences, UCLA, 595 Charles Young Drive, Los Angeles, California 90095, USA. †Present address: School of Earth and Environmental Sciences, University of Portsmouth, Burnaby Road, Portsmouth PO1 3QL, UK.

Pervasive maskelynite indicates shock pressures of at least 29 ± 1 GPa and as high as 80 GPa (ref. 8). Baddeleyite grains range in size from $2 \mu\text{m}$ to $30 \mu\text{m}$ in the longest dimension, and occur as euhedral to subhedral elongate to blocky grains intergrown with, or at the boundaries of, larger main-phase minerals, occasionally near quenched melt pockets (such as Grain 16; see Fig. 1 and Supplementary Figs 1 and 3).

Scanning electron microscopy/cathodoluminescence imaging of submicrometre variations in trace-element chemistry revealed several zoning types. Most grains exhibit narrow, bright blue rims surrounding a dark core of weak, broadly concentric, discontinuous, linear zoning. A subset of grains, often with subhedral to euhedral outlines, exhibits oscillatory planar growth banding that is parallel to straight grain margins or forms triangular sector zoning (Fig. 1b). We report similar sector zoning in igneous micro-baddeleyite from an unshocked terrestrial gabbro sill (Supplementary Fig. 2). Common to the exterior surfaces of many grains is a discontinuous and very narrow rim of zircon, up to a few micrometres in width, identified initially by X-ray energy mapping and confirmed by EBSD (Fig. 1c, d; Supplementary Table 1). In many cases the zircon also fills thin fractures within the micro-baddeleyite. Zircon luminesces in the ultraviolet range and has replaced baddeleyite or grown outward from the baddeleyite grain margin along shock microstructures attributable to post-shock decompression⁷.

Structural alteration of the baddeleyite grains by shock is indicated by high-magnification secondary electron and backscatter electron imaging of grain interiors, which reveals roughly equant granules with diameters of about $0.1 \mu\text{m}$ or less (see Fig. 1a). Electron diffraction patterns are sensitive to lattice disorder, as seen in Apollo lunar zircon¹⁸, and here EBSD mapping at maximum resolution (50 nm) indicates that baddeleyite crystallinity is degraded, and lattice orientation is variable, at length scales below 50 nm. The grains appear nearly as amorphous as the host maskelynite glass (Fig. 1d) generated by the Martian impact and launch

event⁸. The only unshocked mineral identified, other than quenched melt pockets, are the zircon rims that crystallized around shocked micro-baddeleyite. High-magnification backscatter electron and EBSD analysis of the zircon (Fig. 1d; Supplementary Table 1) failed to show any evidence of shock microstructures such as planar features, curvilinear features, shock microtwins¹⁵ or reidite (the high-pressure ZrSiO_4 polymorph). Low-magnification imaging of baddeleyite Grain 16 reveals a spatial correlation between the site of zircon growth and the Si-enriched margin of a quenched melt pocket (Supplementary Fig. 3), the latter a common feature of this strongly shock-heated and rapidly cooled shergottite.

SIMS analysis ($n = 20$; all uncertainties at 2σ confidence level) of 15 grains of partially amorphous baddeleyite, all but one (G2457) rimmed by post-shock zircon, revealed relatively low U abundance (about 50 parts per million, p.p.m., to 300 p.p.m.) compared to the reference standard, and proportions of radiogenic Pb that range widely from 97% to 19% (Supplementary Table 2). The U–Pb data (corrected for common Pb measured in neighbouring minerals) form an array parallel to the Tera–Wasserburg concordia, ranging between 227 ± 18 million years (Myr) and 22 ± 2 Myr in apparent age (Fig. 2, Supplementary Table 2), indicative of varying degrees of recent Pb loss. A broad correlation exists between microstructure and $^{206}\text{Pb}/^{238}\text{U}$ dates in that the four grains with preserved igneous zoning are among the six oldest baddeleyite dates, with the oldest grain (G2457), which is unzoned and intergrown with pyroxene, lacking a reaction rim of post-shock zircon. Together, these data are characteristic of an igneous population of uniform age which has experienced variable degrees of recrystallization, reaction to zircon, and single-stage Pb loss during locally intense shock metamorphism.

Our best estimate of the magmatic crystallization age is obtained from the three grains which yielded both the oldest and least disturbed $^{206}\text{Pb}/^{238}\text{U}$ dates (169 ± 16 Myr to 227 ± 18 Myr) and also the highest

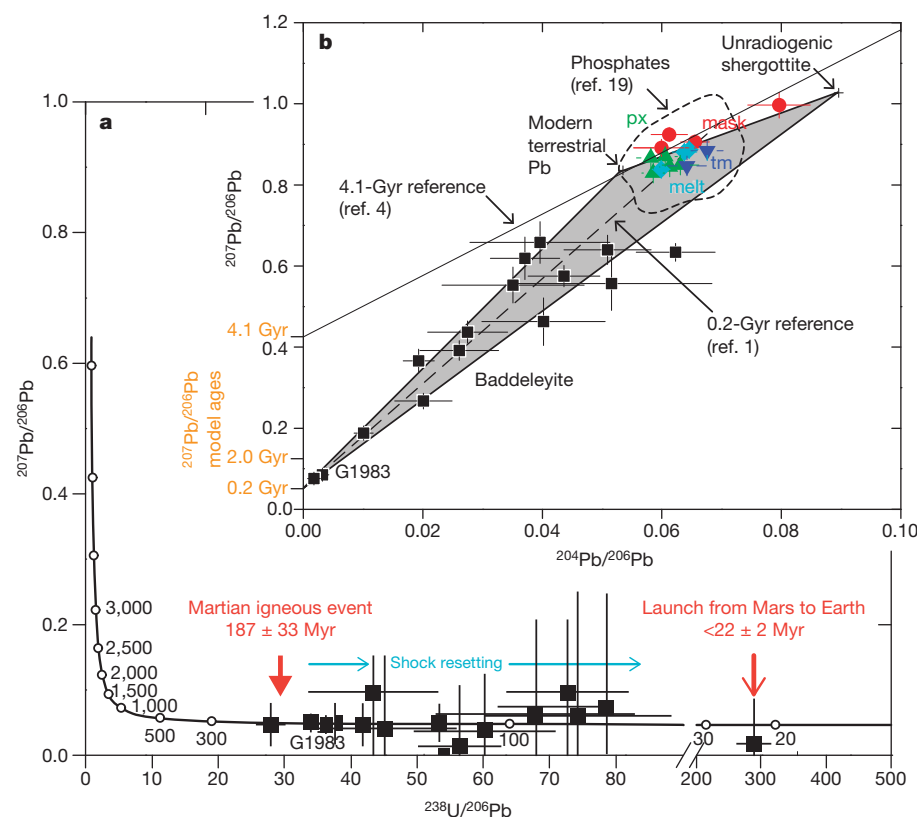


Figure 2 | U–Pb and Pb–Pb (inset) plots of isotopic data (2σ confidence level) for baddeleyite and neighbouring igneous minerals indicating a young crystallization age, variable age disturbance by shock, and inherited primitive Martian Pb. a, Tera–Wasserburg concordia plot of *in situ* SIMS U–Pb baddeleyite data ($n = 20$), corrected for common Pb (see Methods). The original age of the population is interpreted to be 187 ± 33 Myr, based on the weighted $^{206}\text{Pb}/^{238}\text{U}$ dates of the four oldest, most radiogenic analyses, such as G1983 (Supplementary Table 2), with younger grains exhibiting partial Pb loss owing to shock less than 22 ± 2 Myr ago. b, Pb–Pb plot of uncorrected Pb measurements ($n = 15$) from the same baddeleyites (see G1983) compared with SIMS measurements of neighbouring phases (mask, maskelynite; px, pyroxene; tm, titanomagnetite; melt, quenched melt pocket). The baddeleyite Pb–Pb isotopic ratios are insensitive to Pb loss during shock, and are clearly incompatible with a 4.1-Gyr crystallization age, but overlap the 0.2-Gyr isochron originally determined for Shergotty (dashed line). $^{207}\text{Pb}/^{206}\text{Pb}$ model ages are given on the y axis. The scalene triangular distribution reflects mixing of radiogenic, modern terrestrial Pb and a primitive Martian Pb (the reference non-radiogenic Pb composition for depleted shergottite²⁰ is shown). The SIMS common Pb isotopic data for igneous minerals are consistent with arrays of solution and phosphate Pb determined by others^{4,19}, and are a signature of mixing of modern terrestrial Pb with Pb from an ancient U-depleted reservoir unique to Mars^{1,9} that was inherited by the 187 ± 33 -Myr-old magma and NWA 5298.

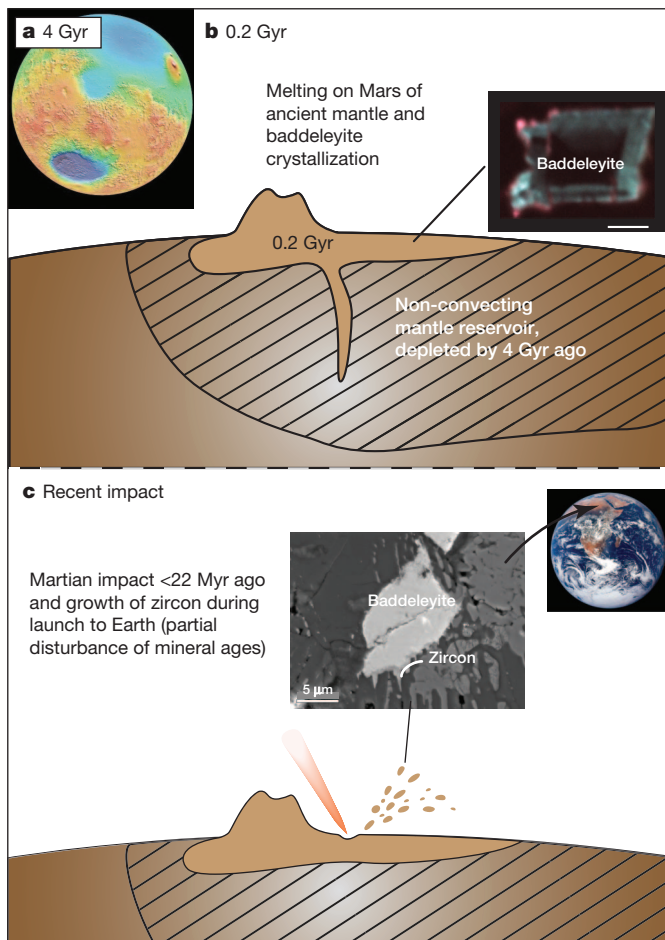


Figure 3 | Three-stage evolution of Martian crust recorded by basaltic shergottite NWA 5298, based on geochemical and nanostructural observations. **a**, Digital elevation map of Mars showing the hemispheric dichotomy caused by an early giant impact²² about 4 Gyr ago, which is one of the processes that may have preserved extremely depleted, ancient mantle reservoirs. **b**, An igneous event at 187 ± 33 Myr (0.2 Gyr) sourced by non-convecting, depleted mantle, most probably due to endogenic hotspot volcanism (for example, Tharsis Montes). The inset shows igneous cathodoluminescence zonation in micro-baddeleyite in the region of NWA 5298 least affected by the later shock event (scale bar, 5 μm). **c**, Spallation of parent body of meteorite NWA 5298 and other ejecta by oblique impact on Mars at some time after 22 ± 2 Myr ago. The second inset shows ejecta zircon filling shock microstructures (scale bar, 5 μm) owing to shock-triggered Si release during cooling and the launch toward Earth (Supplementary Fig. 2).

proportions of radiogenic Pb (68% to 96%), such that the $^{206}\text{Pb}/^{238}\text{U}$ dates are least affected by uncertainty in the common Pb correction. On the basis of the weighted mean of the $^{206}\text{Pb}/^{238}\text{U}$ dates ($n = 4$), the best interpretation of the age of baddeleyite and Martian magma crystallization is 187 ± 33 Myr (Fig. 2a). This is consistent with many mineral isochrons from previous studies such as the value of about 200 Myr obtained from high-precision measurements for Shergotty, Zagami and EETA 79001 (ref. 1) (Fig. 2b) and more recent, less precise laser and ion probe results for phosphates or baddeleyite in other shergottites^{5,6,19}. The Pb–Pb data for baddeleyite have a scalene triangular distribution (Fig. 2b) that indicates three-component mixtures of radiogenic Pb with terrestrial common Pb and Martian common Pb from surrounding mineral phases and surfaces. The y -axis intercept of this distribution corresponds to $^{207}\text{Pb}/^{206}\text{Pb}$ model ages of 419 Myr and 0 Myr if regressed through fixed end-member compositions of the most non-radiogenic known Martian Pb (ref. 20) and modern terrestrial Pb, respectively (Fig. 2b). The associated model age uncertainties are comparatively large (hundreds of millions of years) with respect to

the U–Pb geochronology, yet the data are useful for resolving the age conundrum in that they are insensitive to shock-induced isotopic disturbance, and are clearly impossible with regard to a 4-Gyr crystallization age (Fig. 2b).

The isotopic values of common Pb measured in igneous phases (Supplementary Table 3) are also explicable as mixtures of modern terrestrial Pb and primitive Martian Pb (Fig. 2b). Values for pyroxene, maskelynite and titanomagnetite, as well as a melt pocket, overlap the linear array defined by mineral and whole-rock Pb–Pb values from all other basaltic shergottites^{4,19,20}, with the least radiogenic Pb value for maskelynite approaching the most primitive known shergottite value²⁰. The slope of the array therefore has no age significance²⁰ except that the primitive Pb composition signifies an ancient fractionation event in the first several hundred million years of Martian evolution^{9,21}. The primitive Pb of NWA 5298 and other shergottites is therefore best explained as a chemical signature inherited from the upper mantle that melted to form the shergottite parent magma, rather than the age of magma crystallization itself²⁰.

Many workers have pointed out that parts of the upper mantle of Mars must have maintained very low $^{238}\text{U}/^{204}\text{Pb}$ values^{1,3,9,20}, and been chemically isolated—resisting convective mixing since early in Martian evolution. Proposed causes of extreme fractionation of early Mars range from crystallization of an early magma ocean to early partial melting of the planet²¹, perhaps influenced by later planet-scale impact melting²² (Fig. 3a). An ancient source for shergottite magmas is further supported by the preservation of early geochemical signatures such as their $^{182}\text{W}/^{184}\text{W}$, $^{142}\text{Nd}/^{144}\text{Nd}$ and $^{187}\text{Re}/^{187}\text{Os}$ isotopic compositions^{10,11,23}. The upper-mantle source region(s) for shergottites²⁴ are therefore ones that have been tectonically static, but punctuated by large volumes of recent, concentrated melting. A good analogue are the flanks of the Tharsis Montes at the equatorial bulge of Mars, among the largest volcanoes in our Solar System²⁵, which are underlain by stationary volcanic super cells that pierce the highly cratered Noachian crust at the edge of the Martian hemispheric dichotomy²⁶ (Fig. 3b). Rayed craters in the Tharsis Montes have been identified by recent remote sensing as candidates for one of the launch sites of basaltic shergottite meteorites²⁷.

The shock metamorphism caused by the launch event resulted in minor to approximately 80% loss of radiogenic Pb from baddeleyite (Fig. 2a), a phenomenon useful for bracketing the age of launch events. Such Pb loss is not anticipated on the basis of shock experiments¹³, which employ time-separated application of static shock and hours of post-shock annealing that, perhaps owing to additional differences in grain size and porosity, do not reproduce the fine-grained shock heating, metasomatic and quench features which we observe. These include the unshocked zircon rims around and within fractures of most of our baddeleyite grains. The absence of the high-pressure polymorph reidite in rim zircon, and the spatial association of zircon with quenched pockets of impact melt (Supplementary Fig. 3) is consistent with genesis from baddeleyite exposed to post-shock silicic fluids in a relatively low-pressure environment—an ideal agent for Pb loss from baddeleyite along high-diffusivity pathways created by shock microstructures.

The Martian origin for shergottites was first suggested on the basis of the signature of Martian atmospheric chemistry trapped in quenched melt pockets²⁸, here genetically associated with meteorite ejection and zircon growth, and it is reasonable to conclude that the zircon grew as the Martian fragment was cooling and exiting the atmosphere (Fig. 3c). Assuming a present atmosphere thickness of 10 km and a typical ejection velocity of 5 km s⁻¹ (ref. 29), the shergottite sample would have experienced localized temperature changes of up to around 2,000 °C (ref. 7) in seconds, with some variation in cooling rate depending on the original size and thermal mass of the ejected body. The rapid pace of events in this scenario is consistent with the local preservation of primary trace-element (cathodoluminescence) zoning in baddeleyites, as well as the extremely thin, micrometre-scale growth of unshocked zircon along shock microstructures (Fig. 3c) which we term “ejectic

zircon". The 22 ± 2 Myr age of the most shock-reset baddeleyite (G1) is therefore an upper limit on launch age and travel time to Earth, complementing existing estimates from cosmic ray exposure dating (see ref. 2 and references therein).

Our integrated microstructural and isotopic analyses allow us to assign specific geologic events to the three stages of Martian geochemical evolution recognized in meteorites since the earliest studies: chemical fractionation of the mantle over 4 Gyr ago, relatively recent melting of that mantle 187 ± 33 Myr ago to cause late-Amazonian basalt magmatism, and a recent launch earthward, perhaps from the flanks of volcanic systems such as Tharsis Montes, triggered by an impact on Mars. Future application of our methodology to Martian meteorites and the broader family of planetary and lunar achondrites promises a more accurate understanding of the inherent, invaluable mineral records of inner Solar System evolution.

METHODS SUMMARY

Micro-baddeleyite grains were located in a petrographic thin section of NWA 5298 by electron beam X-ray mapping. Two subsections were cast in separate epoxy mounts (ROM4 and ROM4b) along with the Phalaborwa baddeleyite standard (2,060 Myr old)³⁰. Electron nanobeam analyses using secondary electron, backscatter electron, cathodoluminescence and EBSD detector systems (Fig. 1) were performed at the University of Western Ontario's Zircon and Accessory Phase Laboratory (ZAPLab) using a Hitachi SU-6600 variable-pressure, field-emission-gun scanning electron microscope according to protocols described elsewhere¹⁵. Electron beam analyses preceded ROM4b SIMS measurements. U–Pb and Pb–Pb *in situ* measurements (ions collected from domains as small as 4 μm) were made with the University of California Los Angeles' CAMECA ims1270 ion microprobe using protocols previously described¹⁷. The proportion of common Pb in NWA 5298 baddeleyite was far higher than that in standards within the same mount (Supplementary Table 2), and in terrestrial and lunar micro-baddeleyite samples measured in the same SIMS session. The elevated common Pb is therefore intrinsic to the Martian sample. The 'blank' common Pb isotopic composition of the baddeleyite was determined from SIMS analysis of neighbouring main-phase minerals and a melt pocket (Supplementary Table 3), and a ²⁰⁸Pb-based method (see Methods) was used to correct for common Pb and determine radiogenic U–Pb ratios (Supplementary Table 2). The determination of the common Pb composition of main-phase minerals by SIMS is described in the Methods.

Full Methods and any associated references are available in the online version of the paper.

Received 27 January; accepted 24 May 2013.

- Chen, J. H. & Wasserburg, G. J. Formation ages and evolution of Shergotty and its parent planet from U–Th–Pb systematics. *Geochim. Cosmochim. Acta* **50**, 955–968 (1986).
- Nyquist, L. E. *et al.* Ages and geologic histories of martian meteorites. *Space Sci. Rev.* **96**, 105–164 (2001).
- Borg, L. & Drake, M. J. A review of meteorite evidence for the timing of magmatism and of surface or near-surface liquid water on Mars. *J. Geophys. Res.* **110**, E12S03 (2005).
- Bouvier, A., Blichert-Toft, J., Vervoort, J. D., Gillet, P. & Albarède, F. The case for old basaltic shergottites. *Earth Planet. Sci. Lett.* **266**, 105–124 (2008).
- Herd, C. D. K., Simonetti, A. & Peterson, N. D. *In situ* U–Pb geochronology of martian baddeleyite by laser ablation MC–ICP–MS. *Lunar Planet. Sci. Conf.* **XXXVIII**, abstr. 1664 (2007).
- Niihara, T. Uranium–lead age of baddeleyite in shergottite Roberts Massif 04261: implications for magmatic activity on Mars. *J. Geophys. Res.* **116**, E12008 (2011).
- El Goresy, A. *et al.* Shock-induced deformation of Shergottites: shock–pressures and perturbations of magmatic ages on Mars. *Geochim. Cosmochim. Acta* **101**, 233–262 (2013).
- Hui, H. *et al.* Petrogenesis of basaltic shergottite Northwest Africa 5298: closed-system crystallization of an oxidized mafic melt. *Meteorit. Planet. Sci.* **46**, 1313–1328 (2011).
- Jagoutz, E. Chronology of SNC meteorites. *Space Sci. Rev.* **56**, 13–22 (1991).
- Brandon, A. D., Walker, R. J., Morgan, J. W. & Goles, G. G. Re–Os isotopic evidence for early differentiation of the martian mantle. *Geochim. Cosmochim. Acta* **64**, 4083–4095 (2000).

- Foley, C. N. *et al.* The early differentiation history of Mars from ¹⁸²W–¹⁴²Nd isotope systematics in the SNC meteorites. *Geochim. Cosmochim. Acta* **69**, 4557–4571 (2005).
- Lapen, T. J. *et al.* A younger age for ALH84001 and its geochemical link to shergottite sources in Mars. *Science* **328**, 347–351 (2010).
- Niihara, T., Kaiden, H., Misawa, K., Sekine, T. & Mikouchi, T. U–Pb isotopic systematics of shock-loaded and annealed baddeleyite: implications for crystallization ages of Martian meteorite shergottites. *Earth Planet. Sci. Lett.* **341–344**, 195–210 (2012).
- Krogh, T. E., Kamo, S. L. & Bohor, B. F. Shock metamorphosed zircons with correlated U–Pb discordance and melt rocks with concordant protolith ages indicate an impact origin for the Sudbury Structure. *Geophys. Monogr.* **95**, 343–353 (1996).
- Moser, D. E. *et al.* New zircon shock phenomena and their use for dating and reconstruction of large impact structures revealed by electron nanobeam (EBSD, CL, EDS) and isotopic U–Pb and (U–Th)/He analysis of the Vredefort dome. *Can. J. Earth Sci.* **48**, 117–139 (2011).
- Chamberlain, K. R. *et al.* *In situ* U–Pb SIMS (IN-SIMS) micro-baddeleyite dating of mafic rocks: method with examples. *Precamb. Res.* **183**, 379–387 (2010).
- Schmitt, A. K., Chamberlain, K. R., Swapp, S. M. & Harrison, T. M. *In situ* U–Pb dating of micro-baddeleyite by secondary ion mass spectrometry. *Chem. Geol.* **269**, 386–395 (2010).
- Nemchin, A. *et al.* Timing of crystallization of the lunar magma ocean constrained by the oldest zircon. *Nature Geosci.* **2**, 133–136 (2009).
- Sano, Y., Terada, K., Takeno, S., Taylor, L. A. & McSween, H. Y. Ion microprobe uranium–thorium–lead dating of Shergotty phosphates. *Meteorit. Planet. Sci.* **35**, 341–346 (2000).
- Gaffney, A. M., Borg, L. E. & Connelly, J. N. Uranium–lead isotope systematics of Mars inferred from the basaltic shergottite QUE94201. *Geochim. Cosmochim. Acta* **71**, 5016–5031 (2007).
- Borg, L. E., Edmondson, J. E. & Asmerom, Y. Constraints on the U–Pb isotopic systematics of Mars inferred from a combined U–Pb, Rb–Sr, and Sm–Nd isotopic study of the Martian meteorite Zagami. *Geochim. Cosmochim. Acta* **69**, 5819–5830 (2005).
- Nimmo, F., Hart, S. D., Korycansky, D. G. & Agnor, C. B. Implications of an impact origin for the martian hemispheric dichotomy. *Nature* **453**, 1220–1223 (2008).
- Debaille, V., Brandon, A. D., Yin, Q. Z. & Jacobsen, B. Coupled ¹⁴²Nd–¹⁴³Nd evidence for a protracted magma ocean on Mars. *Nature* **450**, 525–528 (2007).
- Brandon, A. D. *et al.* Evolution of the martian mantle inferred from the ¹⁸⁷Re–¹⁸⁷Os isotope and highly siderophile element abundance systematics of shergottite meteorites. *Geochim. Cosmochim. Acta* **76**, 206–235 (2012).
- Neukum, G. *et al.* The geologic evolution of Mars: episodicity of resurfacing events and ages from cratering analysis of image data and correlation with radiometric ages of Martian meteorites. *Earth Planet. Sci. Lett.* **294**, 204–222 (2010).
- Johnson, C. L. & Phillips, R. J. Evolution of the Tharsis region of Mars: insights from magnetic field observations. *Earth Planet. Sci. Lett.* **230**, 241–254 (2005).
- Tornabene, L. L. *et al.* Identification of large (2–10 km) rayed craters on Mars in THEMIS thermal infrared images: implications for possible Martian meteorite source regions. *J. Geophys. Res.* **111**, E10006 (2006).
- Bogard, D. D. & Johnson, P. Martian gases in an Antarctic meteorite? *Science* **221**, 651–654 (1983).
- Head, J. N., Melosh, H. J. & Ivanov, B. A. Martian meteorite launch: high-speed ejecta from small craters. *Science* **298**, 1752–1756 (2002).
- Heaman, L. M. The application of U–Pb geochronology to mafic, ultramafic and alkaline rocks: an evaluation of three mineral standards. *Chem. Geol.* **261**, 43–52 (2009).

Supplementary Information is available in the online version of the paper.

Acknowledgements We acknowledge the generosity of NWA 5298 donor D. Gregory. This project was supported by NSERC Discovery Grants to D.E.M. and K.T.T., a Wyoming NASA Space grant to K.R.C., an NSF EAR/IF grant to the UCLA SIMS laboratory, and postdoctoral funding to J.R.D. from the Government of Canada and the University of Western Ontario's Center for Planetary Science and Exploration. We thank S. Swapp and N. Swoboda-Colberg for assistance locating and imaging SIMS targets, and I. Craig (University of Western Ontario) for graphics art support. We also thank L. Nyquist and A. Brandon for reviews of the manuscript.

Author Contributions All authors contributed to this work. D.E.M., K.R.C. and K.T.T. designed the initial project. All authors conducted portions of either, or both, the fundamental field emission gun–scanning electron microscopy and SIMS data collection. A.K.S., K.R.C., D.E.M. and J.R.D. reduced the isotope data. D.E.M., I.R.B. and J.R.D. reduced the field emission gun–scanning electron microscopy data. D.E.M. wrote the main paper, and all authors discussed the results and commented on the manuscript at all stages.

Author Information Reprints and permissions information is available at www.nature.com/reprints. The authors declare no competing financial interests. Readers are welcome to comment on the online version of the paper. Correspondence and requests for materials should be addressed to D.E.M. (desmond.moser@uwo.ca).

METHODS

Additional SIMS U–Pb analytical details. Analytical conditions followed those described previously^{16,17}, using a primary beam of about 20- μm diameter and oxygen flooding to enhance Pb ionization. Baddeleyite grain lengths ranged from 8 μm to 32 μm , and widths from 2 μm to 12 μm , with aspect ratios as high as 10:1. The CAMECA ims1270 field aperture was set to achieve effective, approximately square, sampling regions of between 4 μm and 8 μm to minimize contributions from host phases. Pb-isotopic fractionation in SIMS is insignificant relative to the level of precision of our measurements, and the agreement between the young Pb–Pb intercept and U–Pb ages (Fig. 2) alleviates any concerns that beam overlap onto phases other than baddeleyite and zircon could have introduced analytical bias⁴. Post-SIMS imaging confirmed that the ion pits were generally well centred on baddeleyite. There is no correlation between $^{206}\text{Pb}/^{238}\text{U}$ date and grain size. Moreover, there is no correlation between percentage radiogenic Pb for an analysis and its Pb peak intensities normalized to the peak intensity for Zr. If the lower radiogenic Pb contents were due to beam overlap with host minerals, then the ratio of Pb content to Zr content would be expected to increase (less Zr from the baddeleyite, more Pb from the host), but this was not observed. Finally, the analyses with the highest Pb/Zr yielded the oldest ages, and those with the lowest Pb/Zr yielded the youngest ages. This trend supports our interpretation that the range in $^{206}\text{Pb}/^{238}\text{U}$ dates reflects varying degrees of loss of radiogenic Pb.

SIMS common Pb correction of micro-baddeleyite U–Pb ages. The abundance of common Pb detected in the unknowns (baddeleyite) was increased relative to terrestrial standard baddeleyite on the same mounts, which necessitated correction

for common Pb derived from two sources—modern terrestrial Pb from the sample surface and Martian Pb intrinsic to the minerals sputtered during micro-baddeleyite SIMS analysis. A procedural common Pb ‘blank’ correction was determined by analysing the main-phase minerals pyroxene, maskelynite and titanomagnetite in mount ROM4b in the vicinity of the dated baddeleyites, using the same run conditions as for micro-baddeleyite unknowns. Monitor species gold was used to track within-run ratio variations with increasing sputtering depth beneath the coated surface, and Pb in a NIST SRM 610 glass cast in the same mount was measured to gauge relative Pb concentrations. An average Pb isotopic composition among all three phases was then determined, weighted by the intensity of the ^{208}Pb peak. The procedural blank composition for the ^{208}Pb -based correction was determined to be $^{208}\text{Pb}/^{206}\text{Pb} = 2.192$ and $^{208}\text{Pb}/^{207}\text{Pb} = 2.548$ (2σ confidence levels of 1.7% and 1.0%, respectively). The ^{204}Pb peak was measured whenever possible, and runs where peak detection showed a >20 p.p.m. deviation between the centring values for $^{94}\text{Zr}_2\text{O}$ and uranium oxide were excluded, such that $^{204}\text{Pb}/^{206}\text{Pb}$ ratios could not be plotted in Fig. 2b.

SIMS measurement of common Pb isotopic composition of NWA 5298. Within-run Pb isotopic ratios and intensities during measurement of main-phase minerals decreased rapidly along with monitor species gold in the first ten of fifty analytical cycles before approaching plateau values. Hence, these plateau values (Supplementary Table 3) are our closest approximation to the Martian Pb isotopic composition of our sample, and indeed our $^{206}\text{Pb}/^{204}\text{Pb}$ and $^{208}\text{Pb}/^{204}\text{Pb}$ ratios of 15.1 and 33.1, respectively, for the least-radiogenic mineral (titanomagnetite) are within the range of whole-rock values for the suite of enriched shergottites⁴.